Journal of System Simulation

Volume 29 | Issue 9 Article 14

6-2-2020

Multi-scale Mesh Saliency with Local Patch Weighted Curvature Entropy

Xiaodong Wang
1. Marine College, Northwestern Polytechnical University, Xi'an 710072, China;;2. National Key Laboratory of Underwater Information Process and Control, Xi'an 710072, China;;

Hongtao Liang
1. Marine College, Northwestern Polytechnical University, Xi'an 710072, China;;2. National Key Laboratory of Underwater Information Process and Control, Xi'an 710072, China;;

Fengju Kang
1. Marine College, Northwestern Polytechnical University, Xi'an 710072, China;;2. National Key Laboratory of Underwater Information Process and Control, Xi'an 710072, China;;

Gu Hao
1. Marine College, Northwestern Polytechnical University, Xi'an 710072, China;;2. National Key Laboratory of Underwater Information Process and Control, Xi'an 710072, China;;

Multi-scale Mesh Saliency with Local Patch Weighted Curvature Entropy

Abstract

Abstract: Mesh saliency is an important geometrical characteristic of 3D mesh model and has been applied in many applications. Inspired by the existing algorithms, *a novel multi-scale saliency detection method based on local patch weighted curvature entropy was proposed*. A local coordinate system and curvature value of each vertex was estimated. An *improved adaptive patch was defined on the tangent plane using accumulated volume of neighborhood*. Furthermore, deviation of the patch of each vertex to their neighborhood was defined as the weight of curvature value. *The Shannon entropy of weighted curvature values of neighbor vertices within a sphere centered at each vertex was defined as their saliency scores*. Comparisons with state-of-the-art methods have shown the competitive performance in computation speed and the advantage in saliency detection ability of our method.

Keywords

adaptive patch, mesh saliency, 3D mesh model, curvature

Recommended Citation

Wang Xiaodong, Liang Hongtao, Kang Fengju, Gu Hao. Multi-scale Mesh Saliency with Local Patch Weighted Curvature Entropy[J]. Journal of System Simulation, 2017, 29(9): 1976-1983.

第 29 卷第 9 期 系统仿真学报© Vol. 29 No. 9
2017 年 9 月 Journal of System Simulation Sep., 2017

Multi-scale Mesh Saliency with Local Patch Weighted Curvature Entropy

Wang Xiaodong[1,2], *Liang Hongtao*[1,2], *Kang Fengju*[1,2], *Gu Hao*[1,2]

(1. Marine College, Northwestern Polytechnical University, Xi'an 710072, China;
2. National Key Laboratory of Underwater Information Process and Control, Xi'an 710072, China)

Abstract: Mesh saliency is an important geometrical characteristic of 3D mesh model and has been applied in many applications. Inspired by the existing algorithms, *a novel multi-scale saliency detection method based on local patch weighted curvature entropy was proposed*. A local coordinate system and curvature value of each vertex was estimated. An *improved adaptive patch was defined on the tangent plane using accumulated volume of neighborhood*. Furthermore, deviation of the patch of each vertex to their neighborhood was defined as the weight of curvature value. *The Shannon entropy of weighted curvature values of neighbor vertices within a sphere centered at each vertex was defined as their saliency scores*. Comparisons with state-of-the-art methods have shown the competitive performance in computation speed and the advantage in saliency detection ability of our method.

Keywords: adaptive patch; mesh saliency; 3D mesh model; curvature

基于局部区块加权曲率熵的多尺度网格显著性

汪小东[1,2]，梁洪涛[1,2]，康凤举[1,2]，顾浩[1,2]

(1. 西北工业大学航海学院，西安 710072；2. 水下信息处理与控制国家级重点实验室，西安 710072)

摘要： 网格显著性是三维网格模型的一个重要几何属性，已应用于许多方向。受现有算法的启发，*提出了一种基于局部区块曲率熵的多尺度显著性检测算法*。针对每个顶点，定义一个局部坐标系并计算该点曲率值；*通过邻域累积体积定义一个改进的自适应区块*，计算该点邻域球内每个邻居点相对于该区块的偏离值，将该值作为相应邻居点曲率的加权值；*将所有邻居点的加权曲率熵作为该点的显著性值*。该算法在时间复杂度方面具有可比较性，在显著性检测能力上占有优势。

关键词： 自适应区块；网格显著性；三维网格模型；显著性
中图分类号：TP391.9 文献标识码：A 文章编号：1004-731X (2017) 09-1976-08
DOI: 10.16182/j.issn1004731x.joss.201709014

Introduction

3D mesh model has become an indispensable approach to virtually represent the reality world nowadays. Neurophysiological researches of human visual system show that human beings shift focal attention to important points or regions when seeing an object [1-2]. Based on this knowledge, the concept mesh saliency was proposed to determine regions attracting more attention compared to their surroundings on the 3D polygonal mesh, which has been applied in

Received：2017-05-20 **Revised**：2017-07-13;
Foundation item：Foundation items: Northwestern Polytechnical University doctoral dissertation Innovation Fund (CX201701);
Biography：Wang Xiaodong (1990-), Male, Yanan, China, Ph.D. research direction is research of system modeling and simulation.

a set of human centered computing applications, including scene lighting[3], good view selection[4-6], mesh smoothing[7-8], object simplification[9-12], etc.

During the last decade, a number of calculation models have been researched for saliency detection. The pioneer paper by Lee[4] proposed to use a center-surround operator on Gaussian-weighted mean curvatures for mesh saliency. Nevertheless, the result saliency map is sensitive to local curvature variances. Soon afterwards a series of patch-based models were constructed, of which Wu [10] defined the patch-based local contrast and global rarity, then linearly combined both criteria scores as mesh saliency. Tao[13] computed saliency through over-segmenting the mesh into patches and ranking the un-salient ones. Liu[14] also adopted an over-segmenting step and modeled the absorbed time of Markov chain as saliency measure. However, the segmented patches strongly depend on the criteria used, and the consistency of mesh saliency between patches is broken. Besides the patches defined as above, Nouri[6,15] defined an adaptive size patch on the tangent plane of mesh vertices. Then the patch filling with local height field was used as a descriptor of vertices. Unlike the patch-based methods, Song[11] debated to make use of log-Laplacian spectral attributes of the mesh rather than local geometric cues to detect salient regions. In this method, global attributes are taken into consideration. However, the essential simplification steps are applied to original 3D mesh, which takes a long computation time.

Recently, Limper[12] modeled mesh saliency as information theory based local curvature entropy. Compared to the state-of-the-art approaches, it shows a competitive detection quality with an order of magnitude speed increase. Whereas this method works well for uniformly distributed triangular meshes, for example the SHREC 2007 watertight meshes[12].

In this paper, inspired by the work of Limper, et al. a more compatible and efficient method is proposed based on local patch weighted curvature entropy. Given a 3D mesh as input, considering an arbitrary vertex on the mesh, we first estimate the curvature and a local coordinate system at this vertex. Then, an adaptive patch improved from the one by Nouri[15] is constructed based on accumulated volume of neighbors of this vertex. We further calculate the weights of curvature values of its neighbors using corresponding patches. Finally, the multi-scale saliency map at this vertex is modeled as the Shannon entropy of local patch weighted curvatures.

1 Multi-scale mesh saliency

Our model for mesh saliency is established upon the Shannon entropy of local patch weighted curvatures. For this purpose, we now consider a mesh represented by $M = \{V, F\}$, where V is the list of vertex and F is the list of face. For a vertex c, the set of vertices within a sphere centered at v_i with radius r is called neighbors of v_i, expressed by $B(v_i, r)$. The following of this section gives our process to construct the multi-scale mesh saliency.

1.1 Estimating local coordinate system

Curvature has been found to be the main source of information on a 3D mesh[12]. It is a local descriptor of vertex on the mesh. The first step of our saliency model is to compute curvatures, etc. Meanwhile, we also estimate the normal vector N_i and two principle vectors T_i^1 and T_i^2 which compose three base vectors of a local coordinate system with c as the origin. There are a number of methods for curvature computation[16-17]. We have tried several and found

https://dc-china-simulation.researchcommons.org/journal/vol29/iss9/14
DOI: 10.16182/j.issn1004731x.joss.201709014

第 29 卷第 9 期 系统仿真学报 Vol. 29 No. 9
2017 年 9 月 Journal of System Simulation Sep., 2017

that the method of Gumhold[17] gives a better result in our situation. In this method, the set of neighbors $B(v_i, r)$ is considered and two quantities are extracted, the centroid c_i and correlation matrix Cov_i, given by

$$c_i = \frac{1}{|B(v_i,r)|}\sum_{v\in B(v_i,r)} v, c_i \in \mathbf{R^3} \quad (1)$$

$$Cov_i = \frac{1}{|B(v_i,r)|}\sum_{v\in B(v_i,r)} (v-c_i)(v-c_i)^t \quad (2)$$

$$Cov_i \in \boldsymbol{R^3}$$

From the eigenvectors and eigenvalues of this correlation matrix, we can estimate the mean curvature C_i, unit normal vector N_i, two orthogonal unit principle vectors $\{T_i^1, T_i^2\}$ which form the 2D tangent plane at v_i.

1.2 Improved adaptive patch

Although curvature is the main local characteristic of vertex on a 3D mesh, the user study by chen et al. [9] shows that curvature alone is not sufficient to characterize the saliency of a vertex or a region. Once the local coordinate system is established as above, we now construct an adaptive patch on the tangent plane of each vertex to quantitatively characterize its distinctiveness to its neighbors. For each vertex v_i on the mesh, its neighbor vertices $v_j \in B(v_i, r)$ are projected onto the 2D tangent plane defined by $\{T_i^1, T_i^2\}$ as shown in Fig. 1. Then, the patch is defined as a bounded rectangle according to the horizontal and vertical limit coordinates (x_1, x_2), (y_1, y_2) of projected vertices on tangent plane. Where (x_1, x_2) is given by

$$\begin{aligned} &v_j' = (v_j - v_i) - |(v_j - v_i)\cdot N_i| N_i \\ &v_j \in B(v_i, r) \\ &x_1 = \mathrm{Min}(v_j' - v_i)\cdot T_i^1 \\ &x_2 = \mathrm{Max}(v_j' - v_i)\cdot T_i^1 \end{aligned} \quad (3)$$

v_j' is the projection point of v_j, and (y_1,y_2) is calculated in a similar method.

The patch is further divided into $l\times l$ cells equally, and then each is filled in with a difference value $h(m, n)$, where m and n are indices of the cells. Finally, a description matrix $\boldsymbol{M}_i^r$ characterizing the difference between v_i and its neighbors $B(v_i,r)$ is obtained, r is the radius of neighborhood sphere. In the paper by Nouri et al. [15], the difference value $h(m, n)$ is defined as accumulated projection heights as follow:

$$h(m,n) = \sum \| v_j - v_j' \|_2 \quad (4)$$

Where v_j' is projection point located in the cell (m, n) and v_j is corresponding neighbor vertex, the operator $\|\cdot\|_2$ represents 2-norm.

Nevertheless, the difference value constructed in this way only takes into account 3D points cloud and ignores the mesh topology. It works well for uniform mesh (e.g. laser scanning meshes). However, important mesh information would be lost for handmade meshes (e.g. modeled by CAD, 3DMAX) in which the triangle distribution is irregular, for example some triangles are stretched or too large. To solve this undesirable effect, we propose a more compatible definition of $h(m, n)$ by taking the topology of neighbor vertex into account. For each neighbor vertex v_j, we construct a local geometry composed of a set of pentahedrons as shown in right of Fig. 1. Each pentahedron corresponds to the geometric space from one of the incident triangles of v_j to the corresponding projection triangle on tangent plane. We denote its volume by Vol_k^j, where k is the index of incident triangle of v_j. Then the definition of $h(m, n)$ is given as

$$h(m,n) = \sum_{j=1}^{NL}\sum_{k=1}^{NI} Vol_k^j \quad (5)$$

NL represents the number of vertices whose projection points are located in the cell (m, n), NI represents the number of incident triangles of v_j.

Considering those cells that no projection point is located in, the difference value $h(m, n)$ is specified as 0.

This improved method for patch construction takes mesh topology into consideration. It differs from the over-segmenting based ones [10,13-14] which break the continuity of mesh saliency, and also the one by Ref [15] that only encapsulates height characteristic.

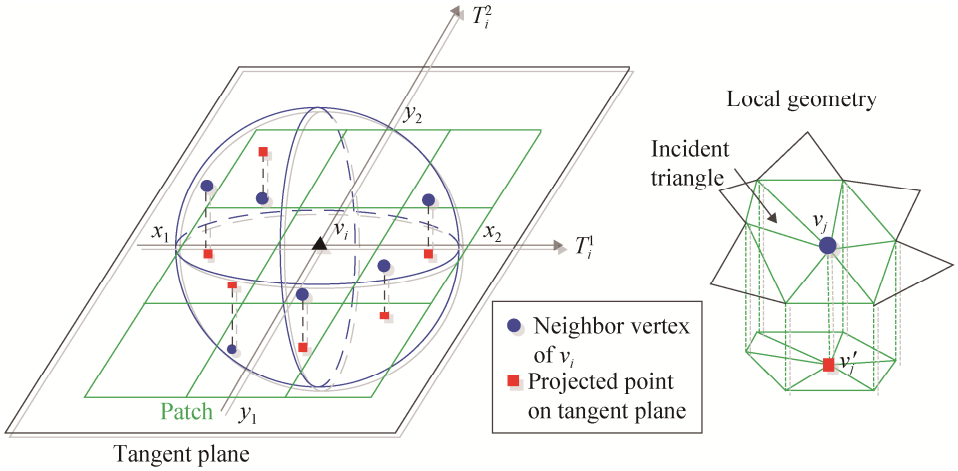

Fig. 1 Illustration of improved adaptive patch

1.3 Shannon entropy based mesh saliency

Shannon entropy [18] is an information theory based concept that measures the uncertainty or average amount of information contained in a message. Assuming that $X=\{x_1,\cdots,x_n\}$ is a discrete random variable with distribution $p_i=Pr[X=x_i]$, i $\in\{1,2,\ldots,n\}$, its Shannon entropy is defined as $H(X)=-\sum_{i=1}^{n} p_i \log p_i$. The base of logarithm is 2 and 0log0 = 0. The unit of entropy is referred as bit.

For each vertex v_i and its neighbor vertex $v_j \in B(v_i,r)$ on the mesh, we now define a variable ω_i with their corresponding description matrices as follow:

$$\overline{\mathbf{M}}=(\mathbf{M}_i^r+\sum_{j=1}^{|B(v_i,r)|}\mathbf{M}_j^r)/(|B(v_i,r)|+1)$$
$$\omega_i=\exp\left[-\left\|\overline{\mathbf{M}}-\mathbf{M}_i^r\right\|_2\right] \quad (6)$$

ω_i is the weight of mean curvature C_i of vertex v_i. Then the local patch weighted curvature of v_i is defined as $\omega_i C_i$, which is a more robust and informative measure compared to curvature by Limper et al [12].

Considering the set of weighted curvature values of v_i and its neighbor vertices, $\phi=\{\omega_i C_i \mid k = i$ or the index of neighbor vertex$\}$, as a message, the local patch weighted curvature entropy can be calculated, we regard this measure as the saliency value of v_i. Like Limper et al., the message ϕ is uniformly sampled into n bins. Then a discrete variable X is obtained. The possibility of X located in each bin is $p_1,\ldots, p_n$ respectively. Then saliency value of v_i is calculated by

$$\text{Saliency}(v_i,r)=H(X)=-\sum_{i=1}^{n} p_i \log p_i \quad (7)$$

The number of bins to discrete saliency values depends on the density of mesh points. It is set to 128 in our experiments.

1.4 Multi-scale mesh saliency

Previous studies on saliency methods have shown that good saliency method should operate at

DOI: 10.16182/j.issn1004731x.joss.201709014

第 29 卷第 9 期 系统仿真学报 Vol. 29 No. 9
2017 年 9 月 Journal of System Simulation Sep., 2017

multiple scales [4]. Since the detected salient regions could be slightly different at different scales. In our implementation, the radius r of neighborhood sphere strongly influences the saliency regions in two aspects. On the one hand, a larger value of r results in larger salient regions on the mesh, for example Fig. 2(a)~(c). On the other hand, locations of the detected salient regions may be different. For example the mouth of bunny model in Fig. 2(b) is not detected as salient region, while it is the opposite in Fig. 2(c).

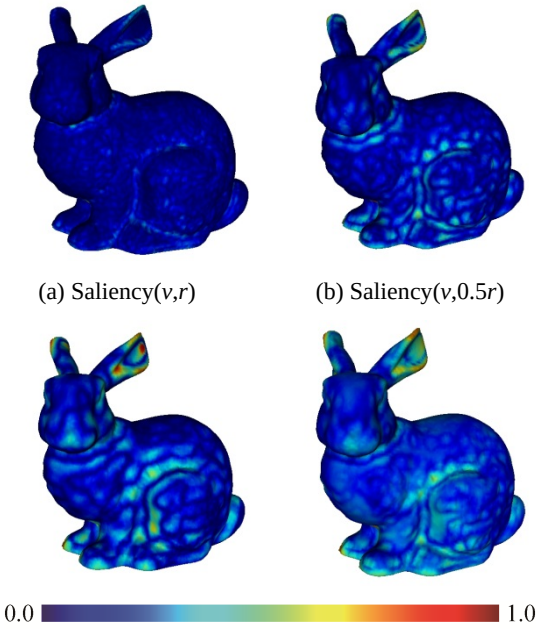

(a) Saliency(v,r) (b) Saliency(v,0.5r)

(c) Saliency(v,0.25r) (d) MS(v_i)

Fig. 2 Saliency maps with different radius of bounding sphere

In order to obtain a multi-scale saliency model that is able to detect as more salient regions included in different scales, we consider the saliency maps with three levels of radius, r, 0.5r, 0.25r, and then averaging them as follow:

$$MS(v_i)=[\text{Saliency}(v_i,r)+\text{Saliency}(v_i,0.5r)+\text{Saliency}(v_i,0.25r)]/3 \quad (8)$$

Finally, a multi-scale saliency model $MS(v_i)$ is established. Fig. 2(d) represents the distribution of final saliency value.

According to a set of previous papers and our experiments, radius r of neighborhood sphere should not exceed an upper limit r_{max}, otherwise the relative salient regions would be covered by its un-salient neighborhoods. It is obvious that r_{max} is related to the size of 3D mesh model. Like Lee et al. [4], we set $r_{max}=\alpha L_d$, where L_d denotes the length of diagonal of bounding box of the model. Experiments in this paper show that a proper value of α is 0.06.

2 Experimental results

In this section, our saliency model is evaluated on a set of 3D mesh models. The test models are from Watertight Track of the SHREC 2007 Shape-based Retrieval Contest[19] and Stanford 3D Scanning Repository. We use the saliency data from user study by Chen[9] as the ground-truth to test and verify the effectiveness of our model. We also compare our model with three state-of-the-art algorithms: Song [11], Limper [12] and Nouri [15]. The tests were performed on a PC with an Intel(R) i5 3.2 GHz processor, 8 GB memory, an NVIDIA graphics card with 4GB memory, and the Open Scene Graph (OSG) engine.

As shown in Fig. 3, we choose a set of representative 3D mesh models from [9] including furniture, animals, instruments and head sculpture. The upper part of Fig. 3 shows the distribution of salient regions of the ground-truth where salient regions are selected by users online, and the under part shows that by our algorithm. It can be intuitively seen that the saliency results detected by our method are basically consistent with the ground-truth. A failed example is the bear model in which the facial features are not detected as saliency by our method since the facial part of the bear model is too flat that does not show abundant geometrical details.

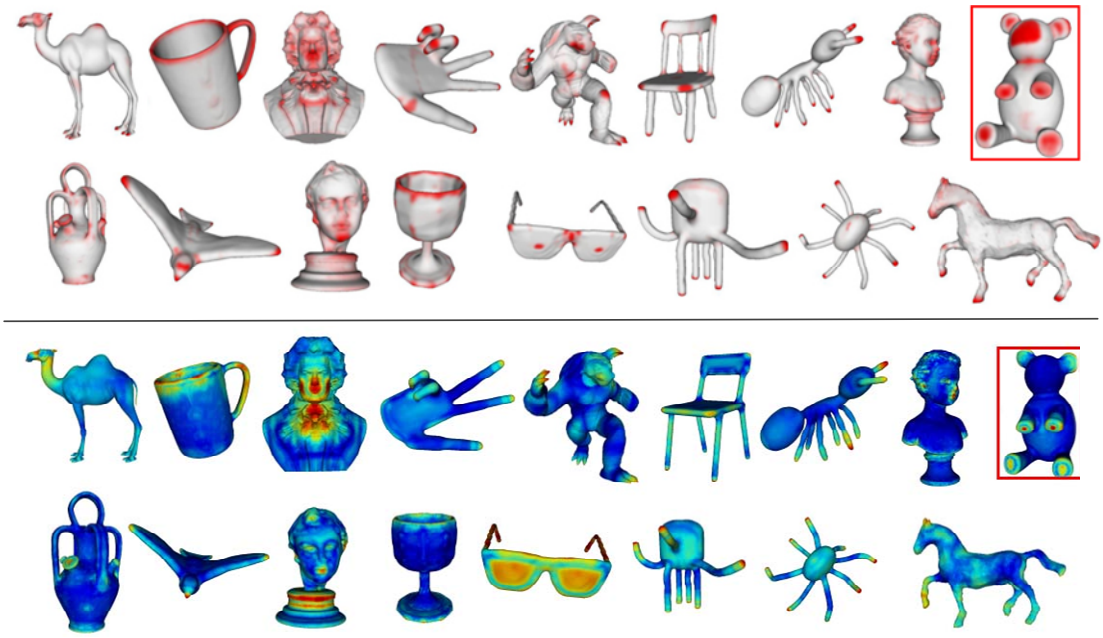

Fig. 3 Comparisons with ground-truth by Chen et al. [9]

In addition to the intuitive comparisons above, the computation times taken by three state-of-the-art methods and ours are also compared. As illustrated in Tab. 1, computation times (in seconds) of six 3D mesh models from Fig. 3 are listed. The algorithm by Song et al. [11] is the most time-consuming due to its simplification process, especially for models with a large number of vertices. And method of Limper et al.[12] exceeds others when considering the computation speed. Compared to this one, our method shows a competitive performance in speed with a little increase of computation time due to the construction process of adaptive patch.

In order to compare the computed saliency values to the ground-truth, we consider the linear correlation coefficient (LCC) between both results as follow

$$LCC(X,Y)=\left|\frac{\mathrm{Cov}(X,Y)}{\sigma_X\sigma_Y}\right| \tag{9}$$

where X is the vector of computed saliency values of a 3D mesh model, Y is the vector of saliency values of the ground-truth, Cov(X,Y) is an operator representing covariance of two variables, σ_X and σ_Y denote the standard deviation of X and Y, respectively. Let $LCC(X, Y) = 0$ if $\sigma_X\sigma_Y = 0$. $LCC(X, Y)$ ranges from 0 to 1 and a higher value means the computed saliency result is closer to the ground-truth. We compute the LCCs between the ground-truth and the computed results by four saliency methods for all 17 mesh models in Fig. 3. The results are plotted as the histogram in Fig. 4 for comparison. And the mean values of LCCs for all the 17 models are 6 163, 5 987, 0.506 2 and 0.545 6 for methods by ours, Song[11], Limper[12] and Nouri[15], respectively. As can be seen, saliency result computed by our method is closer to the ground-truth. In this point, it excels the algorithms of Limper[12] and Nouri[15], since an improved adaptive patch which considers both height fields and incident face areas of neighborhood of each vertex on the mesh is taken into consideration. While the algorithm of Song[11] shows a closer result with ours when compared to the ground-truth, its calculation time is more than ten times of our method if the input mesh consists of dozens of thousands vertices.

https://dc-china-simulation.researchcommons.org/journal/vol29/iss9/14
DOI: 10.16182/j.issn1004731x.joss.201709014

第 29 卷第 9 期 系统仿真学报 Vol. 29 No. 9
2017 年 9 月 Journal of System Simulation Sep., 2017

Tab. 1 Comparisons of computation times with three state-of-the-art methods

Models	#vertices	#triangles	Computation time (second)			
			Nouri [15]	Song [11]	Limper [12]	Ours
Ant	7 038	14 072	5.2	25.6	3.8	5.3
Camel	9 757	19 510	7.3	36.7	6.5	8.9
Horse	11 312	22 620	16.8	48.3	9.4	10.3
Bear	13 867	27 730	21.2	63.1	11.1	13.7
Cup	15 137	30 274	36.4	101.4	15.3	21.0
Boy	25 230	50 456	53.1	452.9	20.7	27.7

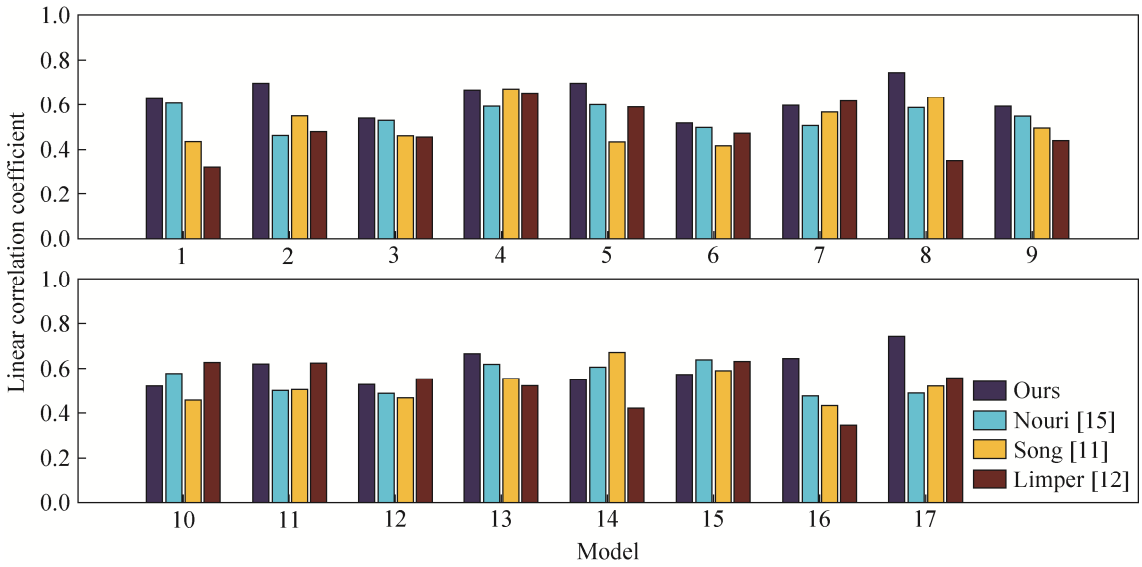

Fig. 4 LCCs between ground-truth and computed values from four methods

3 Conclusions and future work

In this paper, we have presented a novel method to detect saliency regions or points on 3D mesh models. Our approach computes the multi-scale saliency characteristics on the mesh and then combines into a single one. We have also made comparisons with the state-of-the-art methods in both computation speed and correlations with the ground-truth. Experiments on a set of 3D mesh models have shown that the proposed method has a competitive performance in speed compared to that of Ref.[12] and a closer correlation to the ground-truth than the other evaluated methods.

Future work will focus on incorporating global attributes into our saliency scheme. Furthermore, we would also explore the saliency detection of textured mesh models, which can be of high value in real-time rendering applications.

References:

[1] Buschman T J, Miller E K. Top-down versus bottom-up control of attention in the prefrontal and posterior parietal cortices [J]. Science (S0036-8075), 2007, 315(5820): 1860-1862.

[2] Zanto T P, Rubens M T, Thangavel A. Causal role of the prefrontal cortex in top-down modulation of visual processing and working memory [J]. Nature Neuroscience (S1097-6256), 2011, 14(5): 656-661.

[3] Lee C H, Kim Y, Varshney A. Saliency-Guided Lighting [J]. IEICE Transactions on Information & Systems (S1745-1361), 2009, 92(2): 369-373.

[4] Lee C H, Varshney A, Jacobs D W. Mesh saliency [J]. ACM Transactions on Graphics (S0730-0301), 2005, 24(3): 659-666.

[5] Leifman G, Shtrom E, Tal A. Surface regions of interest for viewpoint selection [C]// IEEE Conference on Computer Vision and Pattern Recognition. USA: IEEE, 2012: 414-421.

[6] Nouri A, Charrier C, Lézoray O. Multi-scale mesh saliency with local adaptive patches for viewpoint selection [J]. Signal Processing Image Communication (S0923-5965), 2015, 38: 151-166.

[7] Mao Z, Ma L, Zhao M. A Modified Laplacian Smoothing Approach with Mesh Saliency [M]. Berlin, Heidelberg, Germany: Springer, 2006: 105-113.

[8] Li Z, Ma L, Jin X. A new feature-preserving mesh-smoothing algorithm [J]. The Visual Computer (S1432-2315), 2009, 25(2): 139-148.

[9] Chen X, Saparov A, Pang B. Schelling Points on 3D Surface Meshes [J]. ACM Transactions on Graphics (S0730-0301), 2012, 31(4): 13-15.

[10] Wu J, Shen X, Zhu W. Mesh saliency with global rarity [J]. Graphical Models (S1524-0711), 2013, 75(5): 255-264.

[11] Song R, Liu Y, Martin R R. Mesh saliency via spectral processing [J]. ACM Transactions on Graphics (S0730-0301), 2014, 33(1): 57-76.

[12] Limper M, Kuijper A, Fellner D W. Mesh Saliency Analysis via Local Curvature Entropy [C]// Proceedings of the 37th Annual Conference of the European Association for Computer Graphics: Short Papers, France: Eurographics Association, 2016: 13-16.

[13] Tao P, Cao J, Li S. Mesh saliency via ranking unsalient patches in a descriptor space [J]. Computers & Graphics (S0097-8493), 2014, 46: 264-274.

[14] Liu X, Tao P, Cao J. Mesh saliency detection via double absorbing Markov chain in feature space [J]. The Visual Computer (S0272-1716), 2016, 32(9): 1121-1132.

[15] Nouri A, Charrier C, Lézoray O. Mesh saliency with adaptive local patches [C]// SPIE Electronic Imaging, Three-Dimensional Image Processing, Measurement (3DIPM), and Applications. USA: SPIE, 2015, 9393.

[16] Taubin G. Estimating the tensor of curvature of a surface from a polyhedral approximation [C]// International Conference on Computer Vision. USA: IEEE, 1995: 902-907.

[17] Gumhold S. Feature Extraction from Point Clouds [C]// 2001, Proc. 10th International Meshing Roundtable. USA: Sandia National Laboratories, 2001: 293-305.

[18] Neumann L, Sbert M, Gooch B. Viewpoint quality: Measures and applications [C]// Proceedings of the 1st Eurographics Workshop on Computational Aesthetics in Graphics, Visualization and Imaging. France: Eurographics Association, 2005: 185-192.

[19] Giorgi D, Biasotti S, Paraboschi L. Shape Retrieval Contest 2007: Watertight Models Track [J]. SHREC Competition, 2007, 8(7): 5-10.

https://dc-china-simulation.researchcommons.org/journal/vol29/iss9/14
DOI: 10.16182/j.issn1004731x.joss.201709014